OPTIMIZATION-FREE CONSTRAINED NONLINEAR PREDICTIVE CONTROL - MINERAL PROCESSING APPLICATIONS

Jocelyn Bouchard **,[1] **André Desbiens** **,[1]
René del Villar ***,[1]

LOOP (Laboratoire d'observation et d'optimisation des procédés - Process observation and optimization laboratory)
** *Department of Electrical and Computer Engineering*
*** *Department of Mining, Metallurgical and Materials Engineering*
Université Laval, Pavillon Adrien-Pouliot
Québec (Québec), Canada G1K 7P4
Email: desbiens@gel.ulaval.ca

Abstract: A difficulty with constrained nonlinear control is the minimization of the cost function. With complex system representations such as fundamental models, the required optimization algorithm may be complex to implement, setting its parameters may be difficult and the calculation time may be long. To overcome these problems, an innovative optimization-free predictive control scheme is proposed. The minimization of the cost function is replaced by a simple and easy-to-compute simulation. Two mineral processing applications illustrate the very good performances of this new algorithm.

Keywords: Nonlinear control, multivariable control, predictive control, constraints, optimization.

1. INTRODUCTION

For many nonlinear processes, linear controllers can perform quite adequately. However, nonlinear control can be justified when the plant behavior is highly nonlinear and subject to large and frequent disturbances or when the operating points span a wide range of nonlinear dynamics (Qin and Badgwell, 1997). Furthermore, nonlinear predictive control has to be considered as a solution if safety and actuator constraints exist, which is always the case for real processes.

[1] Partially supported by NSERC (Canada) and FQRNT (Québec).

To describe the dynamic behavior of a process, two possible ways are physical modeling and empirical modeling, both having attractive characteristics and drawbacks (Söderström and Stoica, 1988). Fundamental models are obtained analytically from basic physical laws while empirical modeling is an experimental approach where the parameters of an empirical mathematical relation between the variables of interest are fitted the recorded data. The main drawback of physical models is that some processes are so complex that it is almost impossible to explain their behavior using only first principles. On the other hand, empirical models are much easier to obtain and to use but their parameters do not have any physical meaning and *a priori* information is almost completely neglected. Furthermore, unlike fundamental models, they represent adequately the process only for conditions (operating points, types of inputs, etc.) similar to those found in the recorded data. In fact, if the underlying assumptions of the fundamental models are respected, they can mimic behaviors outside the range of calibration and less data are required for their development.

As a result, fundamental models have been used for nonlinear model predictive control (MPC). However, the considered plants are almost always a single unit operation with a relatively simple dynamic model (Henson, 1998). Writing fundamental models is a difficult task but commercial dynamic simulators are now available. However, using commercial dynamic simulators for nonlinear predictive control (NLPC) does not seem to have been reported yet in the literature (Henson, 1998). The main reason for not using complex fundamental nonlinear models for designing predictive controllers is certainly that the complexity of the on-line solution of the nonlinear programming problem increases with the one of the model, hence leading to computational and reliability difficulties. Another reason why commercial simulators are not used is probably the unavailability of the model equations to the control designer (Henson, 1998).

In recent years, many research works have focused on the nominal stability problem for nonlinear model predictive control. Most proposed solutions consist in insuring nominal stability by imposing penalties or constraints on the terminal state of the prediction horizon (Qin and Badgwell, 1997; Mayne et al., 2000). These solutions are usually computationally quite demanding. Fortunately, algorithms to reduce the computational effort are now appearing in the literature (Fontes, 2001; Magni et al., 2001), but they still remain relatively difficult to implement. However, most nonlinear model predictive controllers do not use terminal state constraints of any kind (Qin and Badgwell, 1997). They instead allow to set the prediction horizon long enough to go beyond the steady-state hence approximating the infinite horizon solution, which leads to nominal stability (Meadows et al., 1995). Therefore, the proposed controller is presented in its simplest form, without relying on terminal state constraints.

The proposed scheme transforms the optimization of the cost function required to solve MPC problems into a control problem. Thus at each sampling time, instead of solving a complex nonlinear programming problem (NLP) to obtain the control action, a simple closed-loop simulation of the process with a pure integrator controller is conducted. The resulting *optimization-by-simulation* (OBS) does not require a NLP solver and is therefore very easy to implement.

Two examples are given to illustrate the method efficiency. The first one shows its use in a constrained multivariable case with an application for the linear control of a grinding circuit. The second one presents the nonlinear control of the cooling zone of an induration furnace where a phenomenological simulator is used as the process model.

2. OPTIMIZATION-FREE CONSTRAINED NONLINEAR PREDICTIVE CONTROL

2.1 Notation

The process inputs and outputs at time $t = k$ are respectively $\boldsymbol{u}(k) \in \Re^n$ and $\boldsymbol{y}(k) \in \Re^n$ (all vectors in the paper are columns). The set points are $\boldsymbol{r}(k) \in \Re^n$. The best plant model M_{Ny}, possibly based on phenomenological relationships and therefore probably highly complex and nonlinear, is described by

$$\boldsymbol{x_{Ny}}(k+1) = \boldsymbol{f_y}\left(\boldsymbol{x_{Ny}}(k), \boldsymbol{u}(k)\right) \quad (1)$$

$$\boldsymbol{y_N}(k) = \boldsymbol{g_y}\left(\boldsymbol{x_{Ny}}(k)\right) \quad (2)$$

Other states or secondary outputs of the plant are denoted $\boldsymbol{w}(k) \in \Re^{n_w}$ where $n_w \leq n$. They can be predicted using the model M_{Nw}

$$\boldsymbol{x_{Nw}}(k+1) = \boldsymbol{f_w}\left(\boldsymbol{x_{Nw}}(k), \boldsymbol{u}(k)\right) \quad (3)$$

$$\boldsymbol{w_N}(k) = \boldsymbol{g_w}\left(\boldsymbol{x_{Nw}}(k)\right) \quad (4)$$

If $n_w < n$, zeros are added to the model to obtain $n_w = n$.

To represent the plant disturbances, the following stochastic model M_S is used

$$\boldsymbol{x_S}(k+1) = \boldsymbol{A_S}\boldsymbol{x_S}(k) + \boldsymbol{B_S}\boldsymbol{\xi}(k) \quad (5)$$

$$\boldsymbol{y_S}(k) = \boldsymbol{C_S}\boldsymbol{x_S}(k) + \boldsymbol{D_S}\boldsymbol{\xi}(k) \quad (6)$$

where $\boldsymbol{\xi}(k) \in \Re^n$ is a zero mean random vector and $\boldsymbol{y_S}(k) \in \Re^n$. The model M_S usually contains an integration to represent non-stationary disturbances hence adding an integral action in the proposed control scheme.

In the following, the notation $\widehat{\boldsymbol{S}}(h : H)$ will refer to the vector of predictions of the signal $\boldsymbol{s}$ over a future horizon $k+h$ to $k+H$

$$\widehat{\boldsymbol{S}}(1:H) = [\ \widehat{\boldsymbol{s}}^T(k+h/k)\ \ \widehat{\boldsymbol{s}}^T(k+h+1/k)\ \ \ldots\ \ \widehat{\boldsymbol{s}}^T(k+H/k)\ ]^T \quad (7)$$

The vector $\boldsymbol{U}(0 : H-1)$ denotes the present and future values of the plant inputs

$$\boldsymbol{U}(0:H-1) = [\ \boldsymbol{u}^T(k)\ \ \boldsymbol{u}^T(k+1)\ \ \ldots\ \ \boldsymbol{u}^T(k+H-1)\ ]^T \quad (8)$$

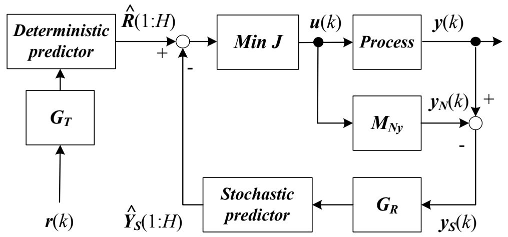

Fig. 1. Control structure

2.2 Controller design

According to a receding horizon procedure, the objective of the proposed method consists in minimizing at each sampling time the following cost function

$$J = [\ \widehat{\boldsymbol{r}}(k+H/k) - \widehat{\boldsymbol{y}}_{\boldsymbol{N}}(k+H/k) \\ -\widehat{\boldsymbol{y}}_{\boldsymbol{S}}(k+H/k)\ ]^2 \tag{9}$$

The minimization of the cost function is subject to a unitary control horizon constraint

$$\boldsymbol{u}(k+i) = \boldsymbol{u}(k) \quad \text{for } i = 1 \text{ to } H-1 \tag{10}$$

and to the following constraints on $\boldsymbol{w_N}$ and $\boldsymbol{u}$

$$\boldsymbol{W_{min}} < \widehat{\boldsymbol{W}}_{\boldsymbol{N}}(1:H) < \boldsymbol{W_{max}} \tag{11}$$

$$\boldsymbol{u_{min}} < \boldsymbol{u}(k) < \boldsymbol{u_{max}} \tag{12}$$

To achieve the above objective, a new predictive control scheme is proposed. The control is calculated by repeating the following procedure at every sampling time. The control structure (Figure 1) is similar to the GlobPC presented by Desbiens et al. (2000) (with the simplification that the tracking and regulation controllers are identical).

Step 1: Measure the process outputs $\boldsymbol{y}(k)$.

Step 2: Estimate the process disturbance with the IMC structure

$$\boldsymbol{y_S}(k) = \boldsymbol{y}(k) - \boldsymbol{y_N}(k) \tag{13}$$

where $\boldsymbol{y_N}(k)$ is calculated with (2).

Step 3: Compute the predictions (details are given in (Desbiens et al., 2000)). Stochastic predictions $\widehat{\boldsymbol{Y}}_s(1:H)$ are calculated using the model M_S and a regulation reference model G_R. Deterministic predictions $\widehat{\boldsymbol{R}}(1:H)$ are based on a tracking reference model G_T. Note that G_T and G_R both have a unitary gain and they respectively modify the tracking and regulation performances.

Step 4: Calculate the control vector action ($\boldsymbol{U}(0:H-1)$) which minimizes the cost function (9) with respect to the constraints (10), (11) and (12). This can be accomplished by using the technique described in Section 2.3.

Step 5: Apply $\boldsymbol{u}(k)$ to the plant.

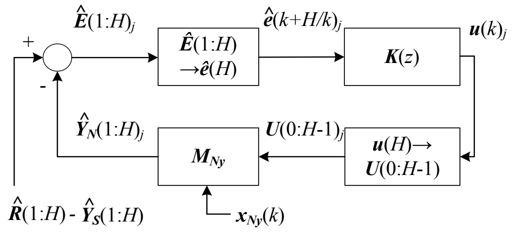

Fig. 2. OBS - without constraints

Step 6: Update the state vectors $\boldsymbol{x}_{Ny}$ and $\boldsymbol{x}_{Nw}$ with (1) and (3). Obviously, better state estimators could be used. Return to Step 1 at the next sampling time ($k = k+1$).

2.3 Optimization-by-simulation

To better understand the OBS approach, the constraints (11) and (12) will first be neglected. Knowing the actual states of M_{Ny}, an integrator controller iteratively calculate different manipulated variables trying to bring $\widehat{\boldsymbol{y}}_{\boldsymbol{N}}(k+H/k)$ equal to $\widehat{\boldsymbol{r}}(k+H/k) - \widehat{\boldsymbol{y}}_{\boldsymbol{S}}(k+H/k)$, hence minimizing the cost function (9). More precisely, every time the cost function must be minimized (at every sampling time k), the system depicted in Figure 2 is simulated until it converges. Each discrete step in the simulation (denoted with the subscript j) is equivalent to an optimization step for usual optimization algorithms. The integrator controller is

$$\boldsymbol{K}(z) = \begin{bmatrix} \frac{K_1}{1-z^{-1}} & 0 & \dots & 0 \\ 0 & \frac{K_2}{1-z^{-1}} & \dots & 0 \\ \dots & \dots & \dots & \dots \\ 0 & 0 & \dots & \frac{K_n}{1-z^{-1}} \end{bmatrix} \tag{14}$$

The block $\widehat{\boldsymbol{E}}(1:H) \longrightarrow \widehat{\boldsymbol{e}}(H)$ extracts the predictions $\widehat{\boldsymbol{e}}(k+H/k)_j$ from its input $\widehat{\boldsymbol{E}}(1:H)_j$, since only the former appears in the cost function and therefore must be integrated. The block $\boldsymbol{u}(H) \longrightarrow \boldsymbol{U}(0:H-1)$ builds the complete vector $\boldsymbol{U}(0:H-1)_j$ from $\boldsymbol{u}(k)_j$ by respecting the control horizon constraint (10). At every simulation step j, the states of the model M_{Ny} are reset to their actual values $\boldsymbol{x_{Ny}}(k)$ before calculating $\widehat{\boldsymbol{Y}}_N(1:H)_j$ for the sequence of inputs $\boldsymbol{U}(0:H-1)_j$ using (2) and (1); indeed the objective is to find the manipulated variables that bring $\widehat{\boldsymbol{y}}_{\boldsymbol{N}}(k+H/k)_j$ to the set point from its actual (at time k) state $\boldsymbol{x_{Ny}}(k)$.

The value of $\boldsymbol{u}(k)_j$ when steady-state is reached is the result of the cost function minimization, i.e. it corresponds to $\boldsymbol{u}(k)$ that must be applied to the plant. For linear systems, it would be easy to show that the solution is optimal since the integrator controller insures that the outputs reach the set points.

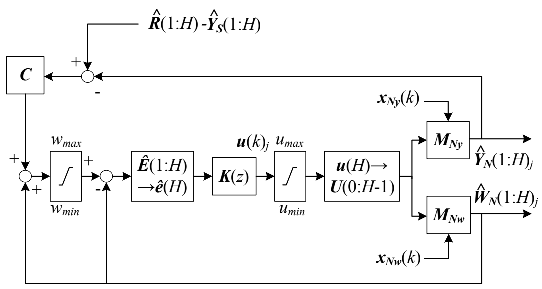

Fig. 3. OBS - with constraints

In presence of constraints, the structure is modified accordingly to the pseudo-cascade approach described by Lestage et al. (1999), as depicted in Figure 3, where $\boldsymbol{C}$ is a diagonal proportional controller. A limiter ensures that the constraints (12) are respected. A second limiter is added for the inner set points, i.e. the set points for $\widehat{\boldsymbol{W}}_{\boldsymbol{N}}(k+H/k)_j$, allowing $\widehat{\boldsymbol{W}}_{\boldsymbol{N}}(k+H/k)_j$ to remain within the constraints $\boldsymbol{W}_{\boldsymbol{min}}$ and $\boldsymbol{W}_{\boldsymbol{max}}$. Momentary or persistent constraint trespassing throughout the prediction horizon may occur in some cases, such as:

- if predictive controller is tuned in such a way that $\widehat{\boldsymbol{W}}_{\boldsymbol{N}}(k+H/k)_j$ inner set points overshooting cannot be avoided (e.g. when H is much shorter than the system settling time)(momentary);
- if M_{Nw} exhibits an important left-half plane zero (momentary);
- if manipulated variable constraints are hit (persistent).

Note that the inner feedback loop is not effective unless saturation occurs, thus ensuring that $\widehat{\boldsymbol{Y}}_{\boldsymbol{N}}(k+H/k)_j$ reaches its set point (unless of course the manipulated variables hit their constraints).

The complete algorithm is the following:

(1) Reset the starting point for the research: $\boldsymbol{u}(k)_0 = \boldsymbol{u}(k-1)$.
(2) Reset the optimization step counter: $j = 1$.
(3) Generate $\boldsymbol{U}(0:H-1)_j$ with $\boldsymbol{u}(H) \longrightarrow \boldsymbol{U}(0:H-1)$ from $\boldsymbol{u}(k)_{j-1}$.
(4) Reset M_{Ny} and M_{Nw} initial conditions: $\boldsymbol{x}_{Ny}(k)_j = \boldsymbol{x}_{Ny}(k)$ and $\boldsymbol{x}_{Nw}(k)_j = \boldsymbol{x}_{Nw}(k)$.
(5) Calculate the corresponding predictions of the models M_{Ny} and M_{Nw}, $\widehat{\boldsymbol{Y}}_N(1:H)_j$ and $\widehat{\boldsymbol{W}}(1:H)_j$, for the sequence of inputs $\boldsymbol{U}(0:H-1)_j$ using (1), (2), (3) and (4).
(6) Following the subsequent sequence of operations of the flowsheet, calculate $\boldsymbol{u}(k)_j$.
(7) Convergence test:
    (a) If the simulation has reached steady-state, then $\boldsymbol{u}(k) = \boldsymbol{u}(k)_j$. Exit and go to step 5 of Section 2.2.
    (b) Else, set $j = j+1$ and go back to step (3).

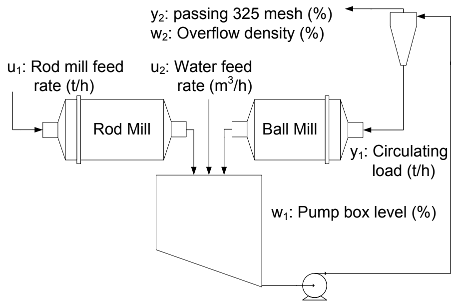

Fig. 4. Grinding circuit

In practice, the convergence test can be selected as follows

$$\|\boldsymbol{u}(k)_j - \boldsymbol{u}(k)_{j-1}\|_2 < \eta\sqrt{n} \tag{15}$$

where $\eta > 0$. The parameter η is therefore the desired precision for the elements of the solution, equivalent to the termination tolerance for usual optimization algorithms.

3. MINERAL PROCESSING APPLICATIONS

3.1 Grinding circuit - Constrained MPC

The purpose of this example is to illustrate how the proposed technique may be used to control a constrained multivariable system. The considered process, a post-classification grinding circuit involving a rod mill and a ball mill, is depicted in Figure 4.

The process outputs are:

- y_1: the circulating load (material fed back to the ball mill in t/h), denoted CL;
- y_2: the size distribution of the overflow (i.e. the *quality* of the product), described by the % passing 325 mesh (47 μm), denoted -325.

Even if it is generally not considered, the circulating load should always be controlled or constrained because mills efficiency decreases drastically outside the optimal range of throughput. In the present case, the circulating load is estimated with a material mass balance around the cyclone using:

$$\omega_F\, x_F = \omega_O\, x_O + \omega_U\, x_U \tag{16}$$

where ω is a pulp flow rate and x, a percent solid. The subscripts F, O, U are respectively used for the feed, overflow and underflow. ω_F, ω_O, x_F and x_O are measured, therefore the circulating load ($\omega_U\, x_U$) may be estimated from (16). Note that the use of a steady-state mass balance is justified because the cyclone dynamics are much faster than the grinding mill dynamics.

In order to insure a proper circuit operation, two other process variables are included as constraints in the control strategy:

- the pump box level (PBL): 25 % $\leq w_1 \leq$ 75 % – to avoid pumping problems and pump box overflows;
- the overflow density (O/FD): 47 % $\leq w_2 \leq$ 53 % – required for upstream processes and to avoid underflow roping.

Only two process variables can be manipulated to control the circuit:

- the rod mill feed rate (RMF) in t/h (u_1);
- the water feed rate (WF) in m^3/h (u_2).

The process is described by the following models M_{Ny} and M_{Nw} (Lestage et al., 1999)

$$\boldsymbol{y_N}(s)=\begin{bmatrix} \frac{13,8}{(1+5700s)(1+400s)} & \frac{4,2(1-700s)}{(1+5000s)(1+5s)} \\ \frac{-0,2(1-900s)e^{-600s}}{(1+5200s)(1+750s)} & \frac{0,012(1+39500s)}{(1+4400s)(1+50s)} \end{bmatrix}\boldsymbol{u}(s) \quad (17)$$

$$\boldsymbol{w_N}(s)=\begin{bmatrix} \frac{5,749}{(1+5500s)(1+210s)} & \frac{1,962}{(1+4700s)} \\ \frac{0,0255(1-5600s)}{(1+5300s)(1+750s)} & \frac{-0,14(1+4050s)}{(1+3200s)(1+60s)} \end{bmatrix}\boldsymbol{u}(s) \quad (18)$$

with the following operating points:

- $u_{1op} = 142$ t/h;
- $u_{2op} = 85$ m^3/h;
- $y_{1op} = 800$ t/h;
- $y_{2op} = 48$ %;
- $w_{1op} = 60$ %;
- $w_{2op} = 50$ %.

The same models are used for the plant simulation (no process-model mismatch). The sampling period T_s is 200 s and the prediction horizon is $H = 12$. The stochastic model is given by

$$\boldsymbol{y_S}(k) = \left[\frac{1-0,8z^{-1}}{1-z^{-1}}\boldsymbol{I}\right]\boldsymbol{\xi}(k) \quad (19)$$

No reference trajectory filters (G_T and G_R) are used and the OBS is set as follows

$$\begin{aligned} \boldsymbol{K}(z) &= \frac{1}{1-z^{-1}}\begin{bmatrix} 0,1638 & 0 \\ 0 & -6,7248 \end{bmatrix} \\ \boldsymbol{C} &= \begin{bmatrix} 0,0729 & 0 \\ 0 & -2,0407 \end{bmatrix} \\ \eta &= 0,5\mathrm{E}-4 \end{aligned} \quad (20)$$

Figure 5 shows an example of the grinding circuit behavior under control. As expected, the circulating load and the size distribution respect their set point when constrained variables are kept within their upper and lower limits. Note that a slight constraint trespassing occurs for w_1 because of the relatively short prediction horizon and for w_2,

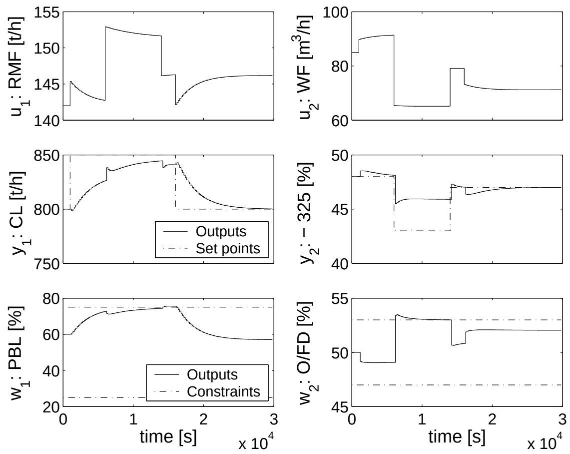

Fig. 5. Constrained CL & size distribution control

because the process has an important left-half plane zero.

3.2 Induration furnace - Unconstrained NLPC

The second example shows how an optimization-free predictive controller may be efficient when based on a phenomenological simulator.

The plant to be controlled is a pellet cooling phenomenological simulator described by Pomerleau et al. (2003). It simulates the cooling zone of an induration furnace used for the agglomeration of iron ore oxide pellets. The two manipulated variables are the shutter positions for two fans forcing the air circulation through the moving bed of pellets (one above and one below). The gas temperature and pressure above the pellet bed are the controlled variables. The simulator is based on energy balance equations for the pellets and the gas. The pressure drop in the bed is calculated with the Ergun's model. The fans characteristics, the pressure drops in the shutters and the pressure loss in the outlet resistance are explained by nonlinear empirical relationships.

The nonlinear model M_{Ny} is identical to the plant. The sampling period is 10 seconds. The horizon is $H = 25$ and the stochastic model is (19). Again, no reference models are used. Figure 6 compares the optimization-free controller (Optim-free) and a nonlinear predictive controller (Optimal) which directly minimizes (9) using lsqnonlin from Matlab. Both approaches lead to similar results but the optimization-free controller allows a significant computation time reduction (about four times faster) for similar termination tolerances.

4. CONCLUSION

A new constrained nonlinear predictive controller is presented and simulation examples illustrate

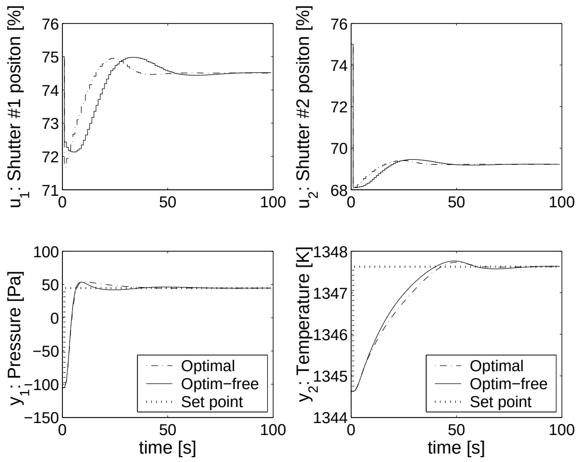

Fig. 6. Nonlinear cooling zone control

its very good performances in terms of efficiency, optimality and computation time.

The novelty of the proposed scheme lies in the computation of the control action at each sampling time period. The optimization of the cost function is replaced by a simulation of the process in closed-loop with an integral controller, using a pseudo-cascade scheme.

The main advantages of using the proposed optimization-free predictive controller are:

- A nonlinear programming solver is not required.
- A phenomenological simulator may easily be used as the process model.
- It is easy to tune: the only parameters to select are the gains of the OBS controllers and η.
- It converges rapidly.

With the optimization-free controller, the optimization problem is seen as a decentralized control problem. This means that as well as the selection of the pairing, the choice of the optimizer gains ($\boldsymbol{C}$ and $\boldsymbol{K}$) are issues that cannot be avoided by further investigations. How the OBS structure deals with constraints incompatibility and how the solutions are affected in term of optimality in such a case remain also to be studied. In other words, neither the convergence conditions nor the optimality of the solutions reached with the OBS technique have been studied yet. A complete analysis is required to evaluate its properties and limitations. Nevertheless, the OBS approach could become a useful and practical solution for constrained nonlinear multivariable predictive control design.

REFERENCES

A. Desbiens, D. Hodouin, and É. Plamondon. Global predictive control: A unified control structure for decoupling setpoint tracking, feedforward compensation and disturbance rejection dynamics. *IEE Proceedings on Control Theory and Applications*, 147:465–475, 2000.

F.A.C.C. Fontes. A general framework to design stabilizing nonlinear model predictive controllers. *Systems & Control Letters*, 42:127–143, 2001.

M.A. Henson. Nonlinear model predictive control: Current status and future directions. *Computers & Chemical Engineering*, 23:187–202, 1998.

R. Lestage, A. Pomerleau, and A. Desbiens. Improved constrained cascade control for parallel processes. *Control Engineering Practice*, 7:969–974, 1999.

L. Magni, G. De Nicolao, and L. Magnani. A stabilizing model-based predictive control algorithm for nonlinear systems. *Automatica*, 37: 1351–1362, 2001.

D.Q. Mayne, J.B. Rawlings, and C.V. Rao. Constrained model predictive control: Stability and optimality. *Automatica*, 36:789–814, 2000.

E.S. Meadows, M.A. Henson, J.W. Eaton, and J.B. Rawlings. Receding horizon control and discontinuous state feedback stabilization. *International Journal of Control*, 62:1217–1229, 1995.

D. Pomerleau, D. Hodouin, and É. Poulin. Performance analysis of a dynamic phenomenological controller for a pellet cooling process. *Journal of Process Control*, 13:137–151, 2003.

S.J. Qin and T.A. Badgwell. An overview of nonlinear model predictive control applications. In J.C. Kantor, C.E. Garcia, and B. Carnahan, editors, *Fifth International Conference on Chemical Process Control*, volume 93, pages 232–256, Englewood Cliffs, 1997. AIChE and CACHE.

T. Söderström and P. Stoica. *System identification*, chapter 1. Prentice Hall, New Jersey, 1988.